Original Article

A scoring diagnostic system based on biparametric ultrasound features for prostate cancer risk assessment

Xiu Liu[1,2#^], Hang Zhou[2,3#^], Xinzhi Xu[2,3^], Ying Li[2,3^], Ruixia Hong[2,3^], Kaifeng Huang[2,3^], Hao Shi[2^], Fang Li[1,2,3^]

[1]Chongqing University Cancer Hospital, School of Medicine, Chongqing University, Chongqing, China; [2]Department of Ultrasound, Chongqing University Cancer Hospital, Chongqing, China; [3]Chongqing Key Laboratory for Intelligent Oncology in Breast Cancer (iCQBC), Chongqing University Cancer Hospital, Chongqing, China

Contributions: (I) Conception and design: X Liu, H Zhou, X Xu, Y Li, R Hong, K Huang, H Shi, F Li; (II) Administrative support: F Li; (III) Provision of study materials or patients: R Hong, F Li; (IV) Collection and assembly of data: X Liu, H Zhou, X Xu, Y Li; (V) Data analysis and interpretation: X Liu, H Zhou, X Xu, K Huang, H Shi; (VI) Manuscript writing: All authors; (VII) Final approval of manuscript: All authors.

[#]These authors contributed equally to this work.

Correspondence to: Fang Li. Chongqing University Cancer Hospital, No. 181 Hanyu Rd., Shapingba District, Chongqing 400030, China. Email: lifang0703@cqu.edu.cn.

Background: Ultrasound has advantages in prostate cancer (PCa) detection and biopsy guidance but lacks a comprehensive quantitative evaluation model with multiparametric features. We aimed to construct a biparametric ultrasound (BU) scoring system for PCa risk assessment and to provide an option for clinically significant prostate cancer (csPCa) detection.

Methods: From January 2015 to December 2020, 392 consecutive patients at Chongqing University Cancer Hospital who underwent BU (grayscale, Doppler flow imaging, and contrast-enhanced ultrasound) and multiparametric magnetic resonance imaging (mpMRI) before biopsy were retrospectively enrolled in the training set to construct the scoring system. From January 2021 to May 2022, 166 consecutive patients at Chongqing University Cancer Hospital were retrospectively enrolled in the validation set. The ultrasound system was compared with mpMRI, and the gold standard was a biopsy. The primary outcome was the detection of csPCa in any area with a Gleason score (GS) ≥3+4, and the secondary outcome was defined as a GS ≥4+3 and/or maximum cancer core length (MCCL) ≥6 mm.

Results: Malignant association features in the nonenhanced biparametric ultrasound (NEBU) scoring system included echogenicity, capsule, and gland asymmetrical vascularity. In the biparametric ultrasound scoring system (BUS), the feature of contrast agent arrival time was added. In the training set, the area under the curves (AUCs) of the NEBU scoring system, BUS, and mpMRI were 0.86 [95% confidence interval (CI): 0.82–0.90], 0.86 (95% CI: 0.82–0.90), and 0.86 (95% CI: 0.83–0.90), respectively (P>0.05). Similar results were also observed in the validation set, in which the areas under the curves were 0.89 (95% CI: 0.84–0.94), 0.90 (95% CI: 0.85–0.95), and 0.88 (95% CI: 0.82–0.94), respectively (P>0.05).

Conclusions: We constructed a BUS that showed efficacy and value for csPCa diagnosis as compared with mpMRI. However, in limited circumstances, the NEBU scoring system may also be an option.

^ ORCID: Fang Li, 0000-0001-7090-8215; Xiu Liu, 0000-0003-0134-5812; Hang Zhou, 0000-0002-8214-3456; Xinzhi Xu, 0000-0002-7054-1406; Ying Li, 0000-0001-7352-1446; Ruixia Hong, 0000-0002-6907-4134; Kaifeng Huang, 0000-0002-6328-267X; Hao Shi, 0000-0002-0482-5339.

Keywords: Imaging; biparametric ultrasound (BU); multiparametric magnetic resonance imaging (mpMRI); prostate cancer (PCa); biparametric ultrasound scoring system (BUS)

Submitted Dec 05, 2022. Accepted for publication Mar 31, 2023. Published online Apr 11, 2023.
doi: 10.21037/qims-22-1354
View this article at: https://dx.doi.org/10.21037/qims-22-1354

Introduction

The incidence of prostate cancer (PCa) continues to rise, with an estimated 1.4 million (7.3%) new cancer cases worldwide in 2020 (1). It ranks second in incidence and fifth in mortality globally, and sixth in incidence and seventh in mortality in China (1,2). PCa is multifocal, with guidelines recommending ultrasound-guided systematic biopsy with or without targeted biopsy (3,4). Based on the clinical management and prognosis, PCa can be simply divided into non-clinically significant prostate cancer (non-csPCa) and clinically significant prostate cancer (csPCa) (4). This classification is based on the Gleason score (GS) and maximum cancer core length (MCCL) (5,6). GS is scored based on primary and secondary structure types, which are added together to indicate the degree of PCa malignancy. The relevant guidelines recommend multiparametric magnetic resonance imaging (mpMRI) in patients with elevated prostate-specific antigen (PSA; PSA >4 ng/mL) and/or abnormal digital rectal examination (DRE) (4), and this has yielded cancer detection rates of 38% to 54% for csPCa (7-9). The widespread use of mpMRI benefits from the Prostate Imaging Reporting and Data System (PI-RADS), which mitigates interobserver variability (10). However, it remains difficult to implement mpMRI in some developing countries due to a lack of resources and its high cost (11). Although guidelines also recommend transrectal ultrasound-guided biopsy, this results in inconsistencies in scan and biopsy images (4). Therefore, developing an economical and accurate method to evaluate csPCa and guide biopsy is urgently needed.

For years, ultrasound, including nonenhanced ultrasound (grayscale, Doppler flow imaging, and elastography) and contrast-enhanced ultrasound, has been employed for prostate scans and biopsies, demonstrating promising ability for the detection of PCa (12-15). Grayscale visualizes the heterogeneity and margin of the gland through echogenicity signals, and Doppler flow imaging displays the intensity and distribution of blood flow through color coding. Elastography reflects the stiffness of the gland (12,16), and contrast-enhanced ultrasound dynamically displays microvascular flow after the intravenous injection of contrast agents. In contrast to the poor diagnostic performance of single modality, multiparametric ultrasound, which usually includes grayscale, Doppler flow imaging, contrast-enhanced ultrasound, and elastography, has been reported to provide complementary images, with a higher detection rate (17). The Cancer Diagnosis by Multiparametric Ultrasound of the Prostate (CADMUS) trial assessing multiparametric ultrasound found that it could be an alternative to mpMRI (18). Although several multiparametric ultrasound studies have affirmed the value of elastography in the diagnosis of PCa, there are some associated problems. For instance, strain elastography is operator-dependent (16), and shear wave elastography cannot maintain uniform pressure on the large gland (19). Moreover, there is a lack of quantitative thresholds of Young's modulus to distinguish malignant from benign tissue (20). These issues increase the difficulty of quality control in elastography.

The current research based on multiparametric ultrasound mostly lacks quantitative criteria for the diagnosis of PCa. There are various ultrasound diagnostic systems for the thyroid, breast, and liver (21-23), but not the prostate, while the existing PI-RADS is based on mpMRI. A reason for this is that there are no obvious nodules as in other solid tumors, and lesions are mostly scattered in the prostate, making it difficult to detect PCa. Therefore, constructing a diagnostic model based on various ultrasound features may help clarify the image evaluation criteria and improve the diagnostic efficacy of ultrasound. This study thus focused on ultrasound images of the entire prostate and aimed to establish a biparametric ultrasound (BU) scoring system, consisting of grayscale, Doppler flow imaging, and contrast-enhanced ultrasound, to provide a quantitative diagnostic reference for PCa. We present the following article in accordance with the STARD reporting checklist (available at https://qims.amegroups.com/article/

view/10.21037/qims-22-1354/rc).

Methods

Patients

This study was conducted in accordance with the Declaration of Helsinki (as revised in 2013) and was approved by the Ethics Committee of Chongqing University Cancer Hospital (No. 2019 [177]). All patients provided written informed consent.

Between January 2015 and December 2020, 451 consecutive patients with suspected PCa at Chongqing University Cancer Hospital were retrospectively enrolled in our single-center study. The inclusion criteria were as follows: (I) serum PSA >4 ng/mL or DRE revealing suspicious nodules in the prostate, (II) urologic symptoms suggestive of PCa, (III) application of BU and mpMRI, and (IV) definitive pathological results. The exclusion criteria were as follows: (I) absence of BU (n=10), (II) absence of mpMRI (n=24), (III) refusal to undergo biopsy (n=6), (IV) previous prostate treatment (n=11), and (V) pathological results without a GS (n=8). Finally, 392 patients were enrolled in the training set. From January 2021 to May 2022, 4, 11, 3, 7, and 5 cases in the validation set were excluded due to absence of BU, absence of mpMRI, biopsy refusal, previous prostate treatment, and lack of GS score, respectively. Ultimately, 166 consecutive patients at Chongqing University Cancer Hospital were retrospectively included.

Procedure

BU scans were performed from the apex (within 5 mm from the tip of prostate), middle (the largest plane between the tip and base of prostate), and base (within 10 mm from the bottom of prostate) with the patient in the left-lateral decubitus position using an endocavity probe (PVT-781VTE; Cannon Aplio 500 or i800). BU consisted of grayscale, Doppler flow imaging, and contrast-enhanced ultrasound, and was performed in the axial plane to visualize the prostate sequentially. Doppler flow imaging included color Doppler flow imaging, power Doppler flow imaging, and superb microvascular imaging. For contrast-enhanced ultrasound, the plane was first adjusted to the suspicious area, which was observed under grayscale and/or Doppler flow imaging and followed by scans of the 3 abovementioned planes. If there was no suspicious area, contrast-enhanced ultrasound was performed in these 3 planes sequentially. Subsequently, a 2.4-mL bolus of the SonoVue contrast agent (Bracco) was injected and followed by a 5-mL saline flush, with a 2-minute dynamic video being saved. All mpMRI scans were performed using a 1.5 T (Achieva, Philips Healthcare) or 3.0 T (Magnetom Prisma, Siemens Healthineers) with a multichannel phased-array body coil. The protocol included T2-weighted imaging obtained using 3 planes (axial, sagittal, and coronal), diffusion-weighted imaging obtained with multiple b values (0, 50, and 1,400 s/mm^2), and dynamic contrast-enhanced MRI. The dynamic contrast-enhanced magnetic resonance imaging scan was started at the same time as the gadolinium-based contrast agent injection at a dose of 1.0 mmol/kg body weight and lasted for 5 minutes. There was no fixed order between the BU and mpMRI scans, but the interval between the two was less than 2 weeks. All images were complete, and the acquisition position of each patient was standardized to meet the requirements of clinical diagnostic quality control.

Ultrasound features

According to previous studies (18,24-26), we generalized the ultrasound features as follows: (I) nodule (present, absent), (II) echogenicity (hyperechoic, hypoechoic, isoechoic), (III) echogenicity location (in the peripheral zone, others), (IV) echogenicity margin (irregular, smooth), (V) capsule (ill-defined, clear), (VI) demarcation between the internal and external gland (ill-defined, clear), (VII) gland increased vascularity (1 or more vessel in the gland, capsular and periureteral flow only), (VIII) gland asymmetrical vascularity (present, absent), (IX) nodule vascularity (present, absent), (X) contrast agent arrival time [abnormal (earlier than the internal gland or the opposite side tissue, or synchronous with the internal gland), normal], (XI) perfusion pattern [abnormal (increased enhancement than the adjacent or the opposite side tissue), normal], and (XII) perfusion at the demarcation between the internal and external gland (present, absent).

Image analysis

Ultrasound images were analyzed according to the consensus of 3 operators with more than 3 years of experience and who were trained by an expert radiologist with more than 10 years of experience in prostate images. The operators were blinded to clinical characteristics, mpMRI findings, and pathology results. The mpMRI

images were analyzed according to the consensus of another 3 operators with more than 3 years of experience in prostate images based on PI-RADS version 2 and on a Likert-type score. The operators' experience, volume, and training were the same as those of the ultrasound operators. Similarly, the mpMRI results were blinded in terms of the clinical characteristics, ultrasound findings, and pathology results.

Biopsy

A biopsy was performed within 2 weeks after image scanning, and the pathological results obtained with the gold standard. If a suspicious lesion was found on BU and/or mpMRI, the ultrasound/mpMRI cognitive fusion target biopsy was performed under the transrectal or transperineal route with 1–3 cores by 1 of 2 operators with more than 5 years of experience in prostate biopsy, and this was followed by a 10–12 core systematic biopsy. Biopsies were conducted with biplane endorectal probes using PVL-715RST equipped on Aplio 500/i800 (Canon; Japan) or EUP-U53 equipped on Hi Vision Preirus systems (Hitachi; Japan). The specimens were sent to the pathology department for analysis based on the 2014 International Society of Urological Pathology Consensus Conference (5). The primary outcome was the detection of csPCa in any area with a GS ≥3+4 (27,28). The secondary outcome was the detection of csPCa with definition 1, which was defined as a GS ≥4+3 and/or MCCL ≥6 mm (18).

Statistical analysis

The continuous variables are expressed as medians with interquartile ranges, and the categorical variables are expressed as percentages. Logistic regression analysis was performed to determine the significant features associated with malignancy. All variables with $P<0.05$ in the univariable logistic regression analysis were incorporated into the multivariable logistic regression analysis. Features with $P<0.05$ in the multivariable analysis were included to construct the ultrasound scoring system. The points were assigned based on the regression coefficient of the multivariable logistic regression analysis. The sensitivity, specificity, and area under the curve (AUC) were used to evaluate the diagnostic performance. Differences among the AUCs of systems were compared using the Delong test. $P<0.05$ was considered statistically significant. The Delong test was performed using R 4.1.3 software (The R Foundation of Statistical Computing), the sample size was estimated using PASS 11.0 (NCSS LLC), and other statistical analyses were performed using SPSS 25.0 (IBM Corp).

Results

Participant characteristics

All eligible patients underwent BU and mpMRI scans, and the flowchart is shown in *Figure 1*. Between January 2015 and December 2020, 392 patients (median age 71 years) were enrolled in the training set. The median volume of the prostate was 48.6 mL (*Table 1*). Pathologically, 270 patients were diagnosed as PCa, of whom 242 had a GS ≥3+4, and 236 were identified as csPCa according to definition 1.

From January 2021 to May 2022, 166 patients (median age 71 years) were included in the validation set. The median volume of the prostate was 49.0 mL. Pathologically, 116 patients were diagnosed as PCa, of whom 104 had a GS ≥3+4, and 105 were identified as csPCa according to definition 1 (*Table 1*).

There were no significant differences in the baseline characteristics between the training and validation sets, and no serious adverse events occurred during image scanning and biopsy.

Ultrasound scoring system establishment

Univariable logistic regression was used to analyze the nonenhanced BU (NEBU) features, including nodule, echogenicity, echogenicity location, echogenicity margin, capsule, demarcation between the internal and external gland, gland increased vascularity, gland asymmetrical vascularity, and nodule vascularity. Three were found to be significant factors according to the multivariable logistic regression analysis (*Table 2*). According to the regression coefficient, hyperechoic, ill-defined capsule, and gland asymmetrical vascularity were assigned 1 point, and hypoechoic was assigned 2 points. Hypoechoic was only recorded if both hyperechoic and hypoechoic were present. The NEBU scoring system (NEBUS) was developed based on the sum of the points, which ranged from 1 to 5 (*Figure 2*). The contrast-enhanced ultrasound features were then added to the logistic regression analysis (*Table 3*). In addition to the above 3 nonenhanced ultrasound features, the contrast agent arrival time feature was also included, which was assigned 1 point. The BU scoring system (BUS) was constructed, containing features from both nonenhanced

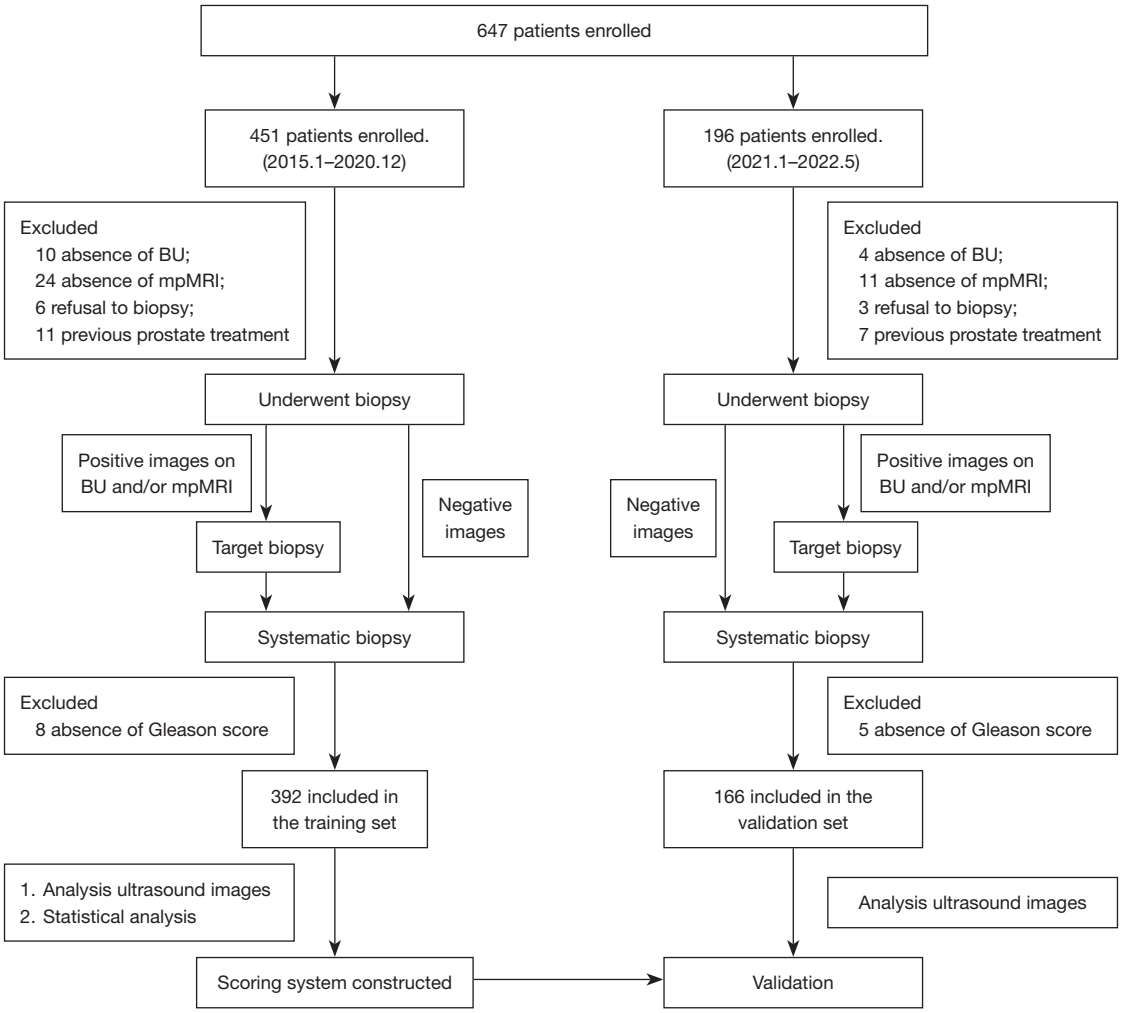

Figure 1 Study and participant selection flow diagram. BU, biparametric ultrasound; mpMRI, multiparametric magnetic resonance imaging.

and contrast-enhanced ultrasound (*Figure 2*).

Diagnostic performance of the systems

The diagnostic performance in the training set is shown in *Tables 4,5*. The cutoff of NEBUS, BUS, and mpMRI was a Likert score ≥3. Using the definition of GS ≥3+4, the sensitivities of NEBUS, BUS, and mpMRI were 97%, 96%, and 96%, respectively. There was no significant difference in the AUCs (P>0.05; *Figure 3A*). According to definition 1, the sensitivities of NEBUS, BUS, and mpMRI were 97%, 96%, and 97%, respectively. The AUC of mpMRI was 0.88 [95% confidence interval (CI): 0.84–0.91] and was not significantly different from the AUCs of 0.86 (95% CI: 0.82–0.90; P>0.05) and 0.87 (95% CI: 0.83–0.90; P>0.05) of NEBUS and BUS, respectively.

In the validation set, NEBUS showed a sensitivity at 95%, BUS at 95%, and mpMRI at 97% under the definition of GS ≥3+4. The BUS showed higher specificity at 65%, followed by NEBUS at 63%, and mpMRI at 39%. Consistent with the results of the training set, there was no significant difference in the AUCs (P>0.05, *Figure 3B*). Under definition 1, the AUCs were 0.87 (95% CI: 0.81–0.92) and 0.88 (95% CI: 0.82–0.93) for NEBUS and BUS, respectively, and were not significantly different from that of mpMRI (0.87; 95% CI: 0.81–0.94; P>0.05).

As shown in *Table 6*, we further grouped PSA according to different ranges to eliminate the deviation caused by a large PSA. PSA levels were divided into group A (PSA <4 ng/mL), group B (PSA 4–<10 ng/mL), group C (PSA 10–20 ng/mL), and group D (PSA >20 ng/mL) (29), with 27, 104, 109, and 318 of 558 patients being placed in each of

Table 1 Participant characteristics in the training and validation sets

Characteristic	Training set (n=392, 70%)	Validation set (n=166, 30%)	P value
Median age, years [IQR]	71 [65–76]	71 [65–76]	0.913
Median PSA, ng/mL (IQR)	24.5 (10.0–55.9)	27.9 (12.1–47.9)	0.971
Median fPSA, ng/mL (IQR)	5.4 (1.7–7.6)	7.5 (2.2–7.5)	0.772
Median fPSA/PSA, (IQR)	0.17 (0.11–0.28)	0.18 (0.11–0.30)	0.783
Median volume, mL (IQR)	48.6 (34.3–74.4)	49.0 (32.7–68.1)	0.960
Pathological result, n [%]			
Benign	122 [31]	50 [30]	
PCa	270 [69]	116 [70]	
Non-csPCa[1†]	150 [38]	62 [37]	
csPCa[1‡]	242 [62]	104 [63]	
Non-csPCa[2§]	156 [40]	61 [37]	
csPCa[2¶]	236 [60]	105 [63]	
Gleason grade, n [%]			
1	28 [10]	12 [10]	
2	25 [9]	11 [9]	
3	30 [11]	18 [16]	
4	93 [34]	31 [27]	
5	94 [35]	44 [38]	

†, the definition of csPCa[1] was the detection of csPCa in any area with a Gleason score ≥3+4; ‡, benign and clinically insignificant prostate cancer (Gleason score <3+4) were included in the non-csPCa[1] group; §, the definition of csPCa[2] was the detection of csPCa, which was defined as a Gleason score ≥4+3 and/or maximum cancer core length ≥6 mm; ¶, benign and clinically insignificant prostate cancer (Gleason score <4+3 and a maximum cancer core length <6 mm) were included in the non-csPCa[2] group. IQR, interquartile range; PSA, prostate-specific antigen; fPSA, free prostate-specific antigen; PCa, prostate cancer; non-csPCa, non-clinically significant prostate cancer; csPCa, clinically significant prostate cancer.

Table 2 Univariable and multivariable logistic regression analyses of the NEBU features

NEBU feature	Univariable analysis		Multivariable analysis	
	β	P value	β	P value
Echogenicity	9.87	<0.001	7.07	<0.001
Echogenicity location	13.22	<0.001		
Echogenicity margin	3.03	<0.001		
Capsule	4.94	<0.001	2.53	0.002
Demarcation	6.62	<0.001		
Nodule	3.11	<0.001		
Gland increased vascularity	4.05	<0.001		
Gland asymmetrical vascularity	7.68	<0.001	2.40	0.006
Nodule vascularity	2.70	0.002		

NEBU, nonenhanced biparametric ultrasound.

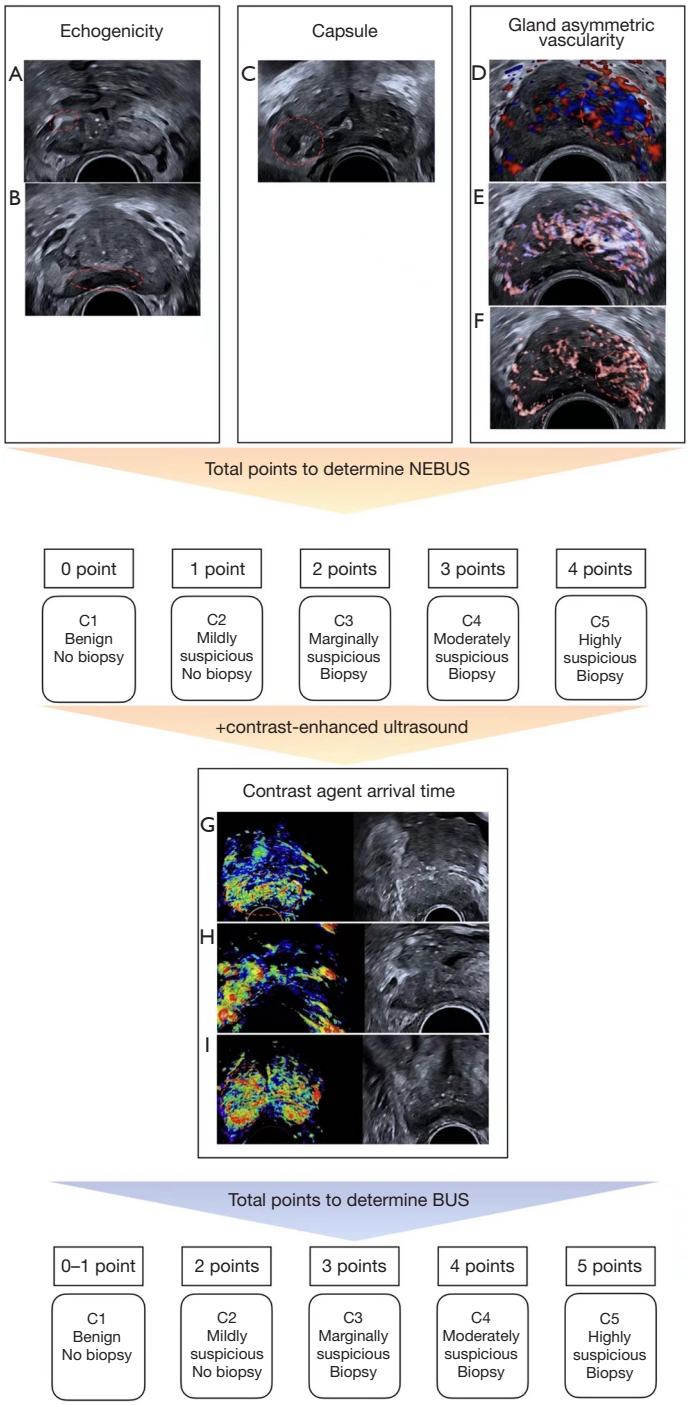

Figure 2 Biparametric ultrasound prostate cancer scoring system with or without contrast-enhanced ultrasound. (A) Hyperechoic in grayscale, assigned 1 point. (B) Hypoechoic in grayscale, assigned 2 points. (C) Ill-defined capsule in grayscale, assigned 1 point. (D-F) Doppler flow imaging showing gland asymmetrical vascularity, assigned 1 point. This feature can be seen in the 3 Doppler images, including color Doppler flow imaging (D), power Doppler flow imaging (E), and superb microvascular imaging (F). The nonenhanced multiparametric ultrasound feature point total indicates the risk level of malignancy. If a contrast-enhanced ultrasound scan is available, we recommend adding it. (G-I) Contrast agent arrival time was assigned 1 point and included 3 abnormal types: (G) contrast agent arrival time earlier than the internal gland, (H) contrast agent arrival time earlier than the opposite side tissue, and (I) contrast agent arrival time synchronous with the internal gland. NEBUS, nonenhanced biparametric ultrasound scoring system; C, category; BUS, biparametric ultrasound scoring system.

Table 3 Univariable and multivariable logistic regression analyses for the BU features

BU feature	Univariable analysis		Multivariable analysis	
	β	P value	β	P value
Echogenicity	9.87	<0.001	6.45	<0.001
Echogenicity location	13.22	<0.001		
Echogenicity margin	3.03	<0.001		
Capsule	4.94	<0.001	2.42	0.005
Demarcation	6.62	<0.001		
Nodule	3.11	<0.001		
Gland increased vascularity	4.05	<0.001		
Gland asymmetrical vascularity	7.68	<0.001	2.19	0.016
Nodule vascularity	2.70	0.002		
Contrast agent arrival time	6.64	<0.001	2.93	0.004
Perfusion pattern	7.31	<0.001		
Perfusion at the demarcation	1.04	0.85		

BU, biparametric ultrasound.

Table 4 The cross-tabulation of BUS and pathology results for csPCa[1] detection in the training set

Diagnostic system	Pathology result		Total	χ^2	P value
	Malignant	Benign			
Training set					
BUS					
Positive	232	56	288	162.78	<0.05
Negative	10	94	104		
Total	242	150	392		
Validation set					
BUS					
Positive	99	22	121	70.08	<0.05
Negative	5	40	45		
Total	104	62	166		

The definition of csPCa[1] was the detection of csPCa in any area with a Gleason score ≥3+4. BUS, biparametric ultrasound scoring system; csPCa, clinically significant prostate cancer.

these 4 groups, respectively. In groups C and D, there was no difference in the AUCs for csPCa detection (P>0.05). In group A, the AUCs of NEBUS and BUS were higher than that of mpMRI regardless of which of the 2 definitions of csPCa was used (P<0.05). In group B, the AUCs of NEBUS and BUS were higher than that of mpMRI according to the definition of GS ≥3+4 (P<0.05).

Discussion

In recent years, mpMRI has been recommended for the detection of csPCa (4,10), but its use is limited by its high

Table 5 Diagnostic performance of the systems in the training and validation sets

Groups	csPCa[1]				csPCa[2]			
	Sen	Spe	Acc (95% CI)	AUC (95% CI)	Sen	Spe	Acc (95% CI)	AUC (95% CI)
Training set								
NEBUS	97%	55%	0.81 (0.77–0.85)	0.86 (0.82–0.90)	97%	53%	0.79 (0.75–0.83)	0.86 (0.82–0.90)
BUS	96%	63%	0.83 (0.79–0.87)	0.86 (0.82–0.90)	96%	61%	0.82 (0.78–0.86)	0.87 (0.83–0.90)
mpMRI	96%	51%	0.79 (0.75–0.83)	0.86 (0.83–0.90)	97%	51%	0.79 (0.75–0.83)	0.88 (0.84–0.91)
Validation set								
NEBUS	95%	63%	0.83 (0.77–0.89)	0.89 (0.84–0.94)	94%	62%	0.83 (0.77–0.88)	0.87 (0.81–0.92)
BUS	95%	65%	0.84 (0.78–0.89)	0.90 (0.85–0.95)	94%	64%	0.83 (0.77–0.89)	0.88 (0.82–0.93)
mpMRI	97%	39%	0.75 (0.69–0.82)	0.88 (0.82–0.94)	97%	39%	0.76 (0.69–0.83)	0.87 (0.81–0.94)

The definition of csPCa[1] was the detection of csPCa in any area with a Gleason score ≥3+4. The definition of csPCa[2] was the detection of csPCa, which was defined as a Gleason score ≥4+3 and/or maximum cancer core length ≥6 mm. csPCa, clinically significant prostate cancer; Sen, sensitivity; Spe, specificity; Acc, accuracy; CI, confidence interval; AUC, area under the curve; NEBUS, nonenhanced biparametric ultrasound scoring system; BUS, biparametric ultrasound scoring system; mpMRI, multiparametric magnetic resonance imaging.

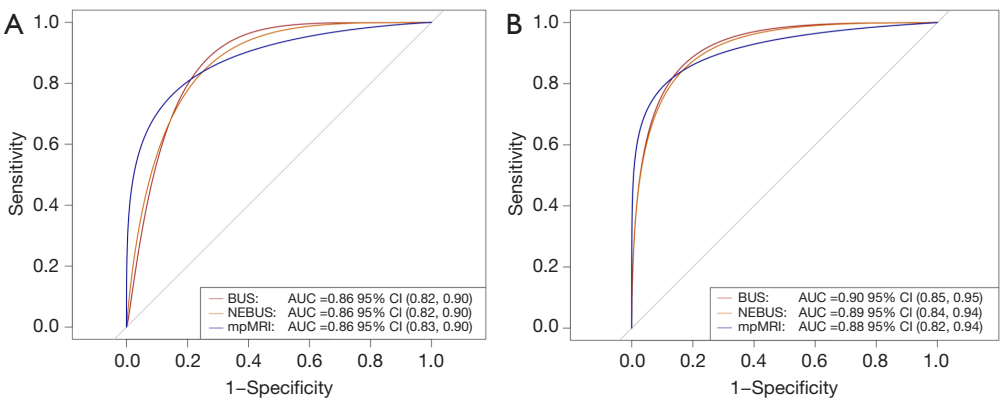

Figure 3 The AUC of the systems for csPCa[1] detection. (A) The AUCs of BUS, NEBUS, and mpMRI in the training set. (B) The AUCs of BUS, NEBUS, and mpMRI in the validation set. The definition of csPCa[1] was the detection of csPCa in any area with a Gleason score ≥3+4. BUS, biparametric ultrasound scoring system; AUC, area under the curve; CI, confidence interval; NEBUS, nonenhanced biparametric ultrasound scoring system; mpMRI, multiparametric magnetic resonance imaging; csPCa, clinically significant prostate cancer.

cost and low specificity (18,30). Ultrasound is economical, real-time, modally diverse, and widely used (17-20). However, an ultrasound system similar to mpMRI PI-RADS is lacking, resulting in the poor repeatability of ultrasound reports. In this study, we explored ultrasound practical features and constructed a quantitative ultrasound scoring system to provide an ultrasound option for PCa risk assessment. Our ultrasound scoring system had a comparable AUC for csPCa detection compared to that of mpMRI. The AUCs of NEBUS and BUS were 0.89 (95% CI: 0.84–0.94) and 0.90 (95% CI: 0.85–0.95), respectively, and the sensitivity of the ultrasound systems (95% in NEBUS and 95% in BUS) was not significantly different from that of mpMRI (97%). However, the specificity of the ultrasound system (63% in NEBUS and 65% in BUS) was better than that of mpMRI (39%).

We constructed a risk-scoring ultrasound system, which included the features of echogenicity, capsule, gland asymmetrical vascularity, and contrast agent arrival time. Grey *et al.* suggested that multiparametric ultrasound

Table 6 The AUCs of the systems in the PSA subgroup

PSA group[I]	csPCa[1]			csPCa[2]		
	NEBUS (95% CI)	BUS (95% CI)	mpMRI (95% CI)	NEBUS (95% CI)	BUS (95% CI)	mpMRI (95% CI)
A	0.86 (0.71–1.00)*	0.86 (0.71–1.00)*	0.68 (0.38–0.98)	0.91 (0.80–1.00)*	0.91 (0.80–1.00) *	0.60 (0.33–0.88)
B	0.80 (0.70–0.89)*	0.84 (0.76–0.92)*	0.68 (0.57–0.80)	0.75 (0.65–0.86)	0.80 (0.70–0.90)	0.73 (0.62–0.83)
C	0.78 (0.69–0.86)	0.77 (0.69–0.86)	0.80 (0.72–0.89)	0.82 (0.75–0.90)	0.82 (0.74–0.90)	0.83 (0.75–0.91)
D	0.87 (0.80–0.94)	0.87 (0.81–0.94)	0.89 (0.82–0.95)	0.82 (0.75–0.89)	0.83 (0.75–0.90)	0.87 (0.81–0.94)

The definition of csPCa[1] was the detection of csPCa in any area with a Gleason score ≥3+4. The definition of csPCa[2] was the detection of csPCa, which was defined as a Gleason score ≥4+3 and/or maximum cancer core length ≥6 mm. [I], group A, PSA <4 ng/mL; group B, 4 ng/mL ≤ PSA < 10 ng/mL; group C, 10 ng/mL ≤ PSA ≤ 20 ng/mL; and group D, PSA >20 ng/mL; *, P<0.05. AUC, area under the curve; PSA, prostate-specific antigen; csPCa, clinically significant prostate cancer; NEBUS, nonenhanced biparametric ultrasound scoring system; CI, confidence interval; BUS, biparametric ultrasound scoring system; mpMRI, multiparametric magnetic resonance imaging.

might have considerable value in the diagnosis of PCa (31), which was confirmed in a subsequent study reporting that multiparametric ultrasound had an equivalent csPCa detection rate to mpMRI (18). Mannaerts *et al.* used a Likert score to evaluate a single ultrasound modality and multiparametric ultrasound using grayscale combined with shear wave elastography and contrast-enhanced ultrasound (17). Their results showed that the sensitivity of the multiparametric ultrasound was 74% for csPCa diagnosis, which was higher than that of the single modality. In their study, the sensitivity of shear wave elastography was 55%, which is not ideal. This may be because of the inability of shear wave elastography to maintain uniform pressure due to signal attenuation on a large prostate (16,17). Additionally, the size of the region of interest is small, resulting in the need for multiple imaging of the whole gland, which makes this examination time-consuming. Although shear wave elastography is often equipped on advanced ultrasound instruments, it still requires a delay in image acquisition to satisfy image quality control (16). Furthermore, a clear cutoff of Young's modulus for distinguishing benign from malignant tissue is also lacking (19,20). Unlike shear wave elastography, which differentiates shear wave speed in tissues, strain elastography displays hardness by detecting strain after external pressure. However, strain elastography is subjective due to the manual pressure applied by the operator and the inconsistent position and size of the region of interest (16). Given the variability of elastography in quality control, elastography was excluded from our study.

The ultrasound features in our study were derived from 3 ultrasound modalities: grayscale, Doppler flow imaging, and contrast-enhanced ultrasound. We developed a quantitative system based on the regression coefficient of ultrasound features, which was similar to the ultrasound system of the breast and thyroid, to provide convenient access and accuracy for prostate risk assessment. Similarly, the ultrasound scoring system had a 5-point score indicating the risk of malignancy (21-23) with the following ranges: category 1 = benign, category 2 = mildly suspicious, category 3 = marginally suspicious, category 4 = moderately suspicious, and category 5 = highly suspicious. Among these, a category ≥3 indicated the need for biopsy. Notably, this system focused on the ultrasound features of the whole prostate rather than the targeted lesion, which makes it possible to manage various PCa situations, including multifocal and diffuse PCa.

To exclude the variability in the degrees of malignancy in patients admitted to the hospital, which could limit the clinical application of the scoring system, we verified that the scoring system applies to the early stage of PCa. We further analyzed 4 PSA subgroups: group A (PSA <4 ng/mL), group B (PSA 4–<10 ng/mL), group C (PSA 10–20 ng/mL), and group D (PSA >20 ng/mL) (32). We found that there were no significant differences in the AUCs of csPCa detection between the ultrasound and mpMRI systems in groups C and D. It is worth noting that the ultrasound system showed better AUCs than did the mpMRI in groups A and B. Meanwhile, the AUCs of the ultrasound system were more uniform across the PSA subgroups than those of mpMRI, indicating that this system may be more reliable for csPCa diagnosis. These results showed that the ultrasound system was not limited by collection bias and demonstrated a stable and efficient diagnostic ability for both early- and late-stage PCa, which attests to its clinical applicability.

Our study had several strengths. First, we developed a quantitative scoring system for PCa risk assessment with simple calculations based on the features of grayscale, Doppler flow imaging, and contrast-enhanced ultrasound. Moreover, this system contained a nonenhanced ultrasound subsystem, which would be more accessible and economical for more grassroots hospitals. Second, the ultrasound system showed a satisfactory diagnostic ability for csPCa compared to mpMRI, especially with PSA <10 ng/mL. Third, only the contrast agent arrival time was considered for contrast-enhanced ultrasound, avoiding the use of additional analysis software. However, there were also some limitations. First, our study was conducted in a cancer hospital, and there was potential for a bias of moderate- and high-risk csPCa, which could have affected the distribution of the csPCa scores. Analyses based on different PSA levels were used to reduce this effect. Second, external validation in a multicenter study with a larger sample size is necessary to reduce the impact of large PSA and verify its clinical practice. Third, a prospective study should be conducted to determine the optimal imaging diagnostic process. Fourth, the biopsy in our study was guided by cognitive fusion, which is dependent on the operator and requires greater anatomical knowledge and spatial sense. Fifth, although elastography was ruled out due to certain limitations, new elastography techniques have gradually emerged and developed into maturity, and we hope to enrich the relevant content in the subsequent experiments of this research series.

Conclusions

We constructed a quantitative BUS for csPCa risk assessment, with or without contrast-enhanced ultrasound. This scoring system can provide an option for clinical practice owing to its accessibility and relatively lower cost. The ultrasound system developed in this study requires further scrutiny and validation before it can be applied in a clinical context.

Acknowledgments

Funding: This work was supported by the Chongqing Technology Innovation and Application Development Project (No. cstc2019jscx-msxmX0099 to F Li); the National Cancer Center Climbing Fund (No. NCC201822B75 to F Li); the Scientific and Technological Research Program of Chongqing Municipal Education Commission (No. KJZD- K202100103 to F Li); and the Natural Science Foundation of Chongqing (No. cstc2020jcyj-msxmX0538 to H Zhou).

Footnote

Reporting Checklist: The authors have completed the STARD reporting checklist. Available at https://qims.amegroups.com/article/view/10.21037/qims-22-1354/rc

Conflicts of Interest: All authors have completed the ICMJE uniform disclosure form (available at https://qims.amegroups.com/article/view/10.21037/qims-22-1354/coif). FL reports that this work was supported by the Chongqing Technology Innovation and Application Development Project (No. cstc2019jscx-msxmX0099), the National Cancer Center Climbing Fund (No. NCC201822B75), and the Scientific and Technological Research Program of Chongqing Municipal Education Commission (No. KJZD-K202100103). HZ reports that this work was supported by the Natural Science Foundation of Chongqing (No. cstc2020jcyj-msxmX0538). The other authors have no conflicts of interest to declare.

Ethical Statement: The authors are accountable for all aspects of the work in ensuring that questions related to the accuracy or integrity of any part of the work are appropriately investigated and resolved. The study was conducted in accordance with the Declaration of Helsinki (as revised in 2013) and was approved by the Ethics Committee of Chongqing University Cancer Hospital (No. 2019[177]). Informed consent was obtained from all individual participants.

References

1. Sung H, Ferlay J, Siegel RL, Laversanne M, Soerjomataram I, Jemal A, Bray F. Global Cancer Statistics 2020: GLOBOCAN Estimates of Incidence and Mortality

Worldwide for 36 Cancers in 185 Countries. CA Cancer J Clin 2021;71:209-49.
2. Xia C, Dong X, Li H, Cao M, Sun D, He S, Yang F, Yan X, Zhang S, Li N, Chen W. Cancer statistics in China and United States, 2022: profiles, trends, and determinants. Chin Med J (Engl) 2022;135:584-90.
3. Løvf M, Zhao S, Axcrona U, Johannessen B, Bakken AC, Carm KT, Hoff AM, Myklebost O, Meza-Zepeda LA, Lie AK, Axcrona K, Lothe RA, Skotheim RI. Multifocal Primary Prostate Cancer Exhibits High Degree of Genomic Heterogeneity. Eur Urol 2019;75:498-505.
4. Mottet N, van den Bergh RCN, Briers E, Van den Broeck T, Cumberbatch MG, De Santis M, et al. EAU-EANM-ESTRO-ESUR-SIOG Guidelines on Prostate Cancer-2020 Update. Part 1: Screening, Diagnosis, and Local Treatment with Curative Intent. Eur Urol 2021;79:243-62.
5. Epstein JI, Amin MB, Reuter VE, Humphrey PA. Contemporary Gleason Grading of Prostatic Carcinoma: An Update With Discussion on Practical Issues to Implement the 2014 International Society of Urological Pathology (ISUP) Consensus Conference on Gleason Grading of Prostatic Carcinoma. Am J Surg Pathol 2017;41:e1-7.
6. Mayer R, Turkbey B, Choyke P, Simone CB 2nd. Combining and analyzing novel multi-parametric magnetic resonance imaging metrics for predicting Gleason score. Quant Imaging Med Surg 2022;12:3844-59.
7. Hofbauer SL, Maxeiner A, Kittner B, Heckmann R, Reimann M, Wiemer L, Asbach P, Haas M, Penzkofer T, Stephan C, Friedersdorff F, Fuller F, Miller K, Cash H. Validation of Prostate Imaging Reporting and Data System Version 2 for the Detection of Prostate Cancer. J Urol 2018;200:767-73.
8. Kasivisvanathan V, Rannikko AS, Borghi M, Panebianco V, Mynderse LA, Vaarala MH, et al. MRI-Targeted or Standard Biopsy for Prostate-Cancer Diagnosis. N Engl J Med 2018;378:1767-77.
9. Yuan J, Poon DMC, Lo G, Wong OL, Cheung KY, Yu SK. A narrative review of MRI acquisition for MR-guided-radiotherapy in prostate cancer. Quant Imaging Med Surg 2022;12:1585-607.
10. Weinreb JC, Barentsz JO, Choyke PL, Cornud F, Haider MA, Macura KJ, Margolis D, Schnall MD, Shtern F, Tempany CM, Thoeny HC, Verma S. PI-RADS Prostate Imaging - Reporting and Data System: 2015, Version 2. Eur Urol 2016;69:16-40.
11. Würnschimmel C, Chandrasekar T, Hahn L, Esen T, Shariat SF, Tilki D. MRI as a screening tool for prostate cancer: current evidence and future challenges. World J Urol 2023;41:921-8.
12. Correas JM, Halpern EJ, Barr RG, Ghai S, Walz J, Bodard S, Dariane C, de la Rosette J. Advanced ultrasound in the diagnosis of prostate cancer. World J Urol 2021;39:661-76.
13. Lee KS, Koo KC, Chung BH. Quantitation of hypoechoic lesions for the prediction and Gleason grading of prostate cancer: a prospective study. World J Urol 2018;36:1059-65.
14. Yang JC, Tang J, Li J, Luo Y, Li Y, Shi H. Contrast-enhanced gray-scale transrectal ultrasound-guided prostate biopsy in men with elevated serum prostate-specific antigen levels. Acad Radiol 2008;15:1291-7.
15. Zhu YC, Shan J, Zhang Y, Jiang Q, Wang YB, Deng SH, Qu QH, Li Q. Prostate Cancer Vascularity: Superb Microvascular Imaging Ultrasonography with Histopathology Correlation. Med Sci Monit 2019;25:8571-8.
16. Cosgrove D, Piscaglia F, Bamber J, Bojunga J, Correas JM, Gilja OH, et al. EFSUMB guidelines and recommendations on the clinical use of ultrasound elastography. Part 2: Clinical applications. Ultraschall Med 2013;34:238-53.
17. Mannaerts CK, Wildeboer RR, Remmers S, van Kollenburg RAA, Kajtazovic A, Hagemann J, Postema AW, van Sloun RJG, J Roobol M, Tilki D, Mischi M, Wijkstra H, Salomon G. Multiparametric Ultrasound for Prostate Cancer Detection and Localization: Correlation of B-mode, Shear Wave Elastography and Contrast Enhanced Ultrasound with Radical Prostatectomy Specimens. J Urol 2019;202:1166-73.
18. Grey ADR, Scott R, Shah B, Acher P, Liyanage S, Pavlou M, et al. Multiparametric ultrasound versus multiparametric MRI to diagnose prostate cancer (CADMUS): a prospective, multicentre, paired-cohort, confirmatory study. Lancet Oncol 2022;23:428-38.
19. Sigrist RMS, Liau J, Kaffas AE, Chammas MC, Willmann JK. Ultrasound Elastography: Review of Techniques and Clinical Applications. Theranostics 2017;7:1303-29.
20. Sarkar S, Das S. A Review of Imaging Methods for Prostate Cancer Detection. Biomed Eng Comput Biol 2016;7:1-15.
21. Tessler FN, Middleton WD, Grant EG, Hoang JK, Berland LL, Teefey SA, Cronan JJ, Beland MD, Desser TS, Frates MC, Hammers LW, Hamper UM, Langer JE, Reading CC, Scoutt LM, Stavros AT. ACR Thyroid Imaging, Reporting and Data System (TI-RADS): White

Paper of the ACR TI-RADS Committee. J Am Coll Radiol 2017;14:587-95.
22. Liberman L, Menell JH. Breast imaging reporting and data system (BI-RADS). Radiol Clin North Am 2002;40:409-30, v.
23. Chernyak V, Fowler KJ, Kamaya A, Kielar AZ, Elsayes KM, Bashir MR, Kono Y, Do RK, Mitchell DG, Singal AG, Tang A, Sirlin CB. Liver Imaging Reporting and Data System (LI-RADS) Version 2018: Imaging of Hepatocellular Carcinoma in At-Risk Patients. Radiology 2018;289:816-30.
24. Lee HJ, Choe GY, Seong CG, Kim SH. Hypoechoic rim of chronically inflamed prostate, as seen at TRUS: histopathologic findings. Korean J Radiol 2001;2:159-63.
25. Bono AV, Celato N, Cova V, Salvadore M, Chinetti S, Novario R. Microvessel density in prostate carcinoma. Prostate Cancer Prostatic Dis 2002;5:123-7.
26. Maxeiner A, Fischer T, Schwabe J, Baur ADJ, Stephan C, Peters R, Slowinski T, von Laffert M, Marticorena Garcia SR, Hamm B, Jung EM. Contrast-Enhanced Ultrasound (CEUS) and Quantitative Perfusion Analysis in Patients with Suspicion for Prostate Cancer. Ultraschall Med 2019;40:340-8.
27. Chu CE, Cowan JE, Lonergan PE, Washington SL 3rd, Fasulo V, de la Calle CM, Shinohara K, Westphalen AC, Carroll PR. Diagnostic Accuracy and Prognostic Value of Serial Prostate Multiparametric Magnetic Resonance Imaging in Men on Active Surveillance for Prostate Cancer. Eur Urol Oncol 2022;5:537-43.
28. Eklund M, Jäderling F, Discacciati A, Bergman M, Annerstedt M, Aly M, Glaessgen A, Carlsson S, Grönberg H, Nordström T; STHLM3 consortium. MRI-Targeted or Standard Biopsy in Prostate Cancer Screening. N Engl J Med 2021;385:908-20.
29. Chapman CH, Caram MEV, Radhakrishnan A, Tsodikov A, Deville C, Burns J, Zaslavsky A, Chang M, Leppert JT, Hofer T, Sales AE, Hawley ST, Hollenbeck BK, Skolarus TA. Association between PSA values and surveillance quality after prostate cancer surgery. Cancer Med 2019;8:7903-12.
30. Drost FH, Osses D, Nieboer D, Bangma CH, Steyerberg EW, Roobol MJ, Schoots IG. Prostate Magnetic Resonance Imaging, with or Without Magnetic Resonance Imaging-targeted Biopsy, and Systematic Biopsy for Detecting Prostate Cancer: A Cochrane Systematic Review and Meta-analysis. Eur Urol 2020;77:78-94.
31. Grey A, Scott R, Charman S, van der Meulen J, Frinking P, Acher P, Liyanage S, Madaan S, Constantinescu G, Shah B, Graves CB, Freeman A, Jameson C, Ramachandran N, Emberton M, Arya M, Ahmed HU. The CADMUS trial - Multi-parametric ultrasound targeted biopsies compared to multi-parametric MRI targeted biopsies in the diagnosis of clinically significant prostate cancer. Contemp Clin Trials 2018;66:86-92.
32. R Zlotta A, V Carlsson S, Finelli A, E Fleshner N. Re: Reconsidering Prostate Cancer Mortality - The Future of PSA Screening: Against increasing PSA threshold to 10 ng/ml. Eur Urol 2020;78:927-9.

Cite this article as: Liu X, Zhou H, Xu X, Li Y, Hong R, Huang K, Shi H, Li F. A scoring diagnostic system based on biparametric ultrasound features for prostate cancer risk assessment. Quant Imaging Med Surg 2023;13(6):3703-3715. doi: 10.21037/qims-22-1354

